

Compensation of refractive dispersion of materials with metasurfaces

A Thesis

submitted to

Indian Institute of Science Education and Research, Pune

in partial fulfilment of the requirements for the

BS-MS Dual Degree Programme

by

Purva Bhumkar



Indian Institute of Science Education and Research, Pune

Dr. Homi Bhabha Road,

Pashan, Pune 411008, INDIA.

April, 2018

Supervisor: Dr. Patrice Genevet

Centre de Recherche sur l'Hétéro-Epitaxie et ses Applications- CNRS, France

© Purva Bhumkar 2018


All rights reserved

Certificate

This is to certify that this dissertation entitled Compensating refractive dispersion of materials with metasurfaces towards the partial fulfilment of the BS-MS dual degree programme at the Indian Institute of Science Education and Research, Pune represents study/work carried out by Purva Bhumkar at Centre de Recherche sur l'Hétéro-Epitaxie et ses Applications, France under the supervision of Dr. Patrice Genevet, Research Scientist, NanoCRHEAtion team, during the academic year 2017-2018.



Purva Bhumkar



Dr. Patrice Genevet

Committee:

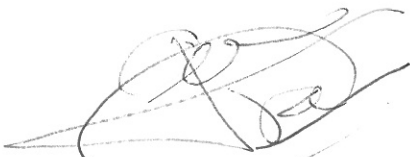
Dr. Patrice Genevet

Dr. G.V. Pavan Kumar

This thesis is dedicated to my parents

Declaration

I hereby declare that the matter embodied in the report entitled Compensating refractive dispersion of materials with metasurfaces are the results of the work carried out by me in the NanoCRHEAtion team at Centre de Recherche sur l'Hétéro-Epitaxie et ses Applications, France under the supervision of Dr. Patrice Genevet and the same has not been submitted elsewhere for any other degree.



Dr. Patrice Genevet



Purva Bhumkar

Acknowledgments

I deeply thank Dr. Patrice Genevet for being a very supportive and dedicated supervisor. I did a summer internship with him in my third year. I feel fortunate that he had the faith in me and gave me another opportunity to work in his group for the thesis project. His efforts towards actively working with me on new experiments and encouraging me to be liberal and independent after the training helped me become confident about my work. His work ethic of guiding and discussing the work on a day to day basis proved extremely important for the progress of my project.

I am grateful to Prof. Federico Capasso's group at Harvard for collaborating with us. Special thanks to Alexander Zhu for preparing samples for my experiments. I thank Postdoctoral fellows, Dr. Peinan Ni and Dr. Sébastien Héron for their valuable suggestions and brainstorming required throughout my work. Many thanks to Peinan for teaching me ellipsometry, fabrication processes and helping me setup Fourier microscopy experiments. I thank doctoral students Gauthier Briere for guiding me in computational techniques, Mario Ferraro for helping me with my doubts and Rajath Sawant for carrying out experiments on my behalf in the later part of the project. I have got amazing support from my lab members Synda, Gustavo, Rami, Roy, Samuel and Victor during my term in France. Discussions with them during lunch breaks ranging from politics to Star Wars have been super fun and mind refreshing.

I thank my TAC member at IISER, Dr. G. V. Pavan Kumar for his motivation and support. I thank CNRS-CRHEA for giving me an opportunity to be a part of it and supporting me financially. I extend my regards to Charap master's program 2017-2018 for providing help with accommodation and insurance facilities in France.

I cannot thank my beloved parents enough for showing belief and courage to send me abroad for my studies; their unconditional love and endless sacrifices always motivate me to become a better version of me and reach newer heights of success in my life.

Abstract

Metasurfaces are a class of two dimensional nano-engineered materials capable of controlling light-matter interaction at interfaces. These materials which are composed of subwavelength phase-shifters can tailor properties of light at will. Today, efforts are taken to improve functionality and minimize the size and weight of optical devices. Metasurfaces being planar, light weight and providing light control are good candidates in revolutionizing a new class of flat optics. This thesis addresses the problem of chromatic aberration in conventional optical components which when ruled out can enhance visible light optical imaging.

Conventional diffractive planar components like flat lenses, diffraction gratings are very much wavelength specific. Such optical components exhibit dispersion phenomenon as the refractive index of the material changes with wavelength. A change in the wavelength then causes focussing problems and chromatic aberrations giving poor image quality. In this thesis, we study the method of compensating for the dispersion of materials by coupling light at the interface of material with metasurfaces.

The study takes into account the dispersive phase compensation approach to achieve achromatic response in optical components. We theoretically show that dispersion of material can be compensated with dispersion of metasurfaces. We experimentally show a single prism turning achromatic, that is, light refracting independent of wavelength because of the modified optical response occurring due to metasurfaces at interface. This achromatic response is achieved for 300 nm visible range bandwidth from 500 to 800 nm. Dispersion of material is measured using Fourier plane imaging microscopy.

The compensation of dispersion being observed in a simple optical component as that of a prism provides motivation for designing achromatic metalenses in the visible range. Since this work addresses the fundamental problem in imaging which is affected by dispersive aberrations, it immediately finds applications in designing broadband visible range achromatic metalenses for imaging systems. These interesting applications towards achieving super-resolved diffraction limited focusing are the major goals regarding the future of this work.

Contents

Abstract

| | | |
|-----|--|----|
| 1 | Introduction | 1 |
| 1.1 | Metasurfaces and flat optics | 1 |
| 1.2 | Problem of chromatic aberration | 2 |
| 1.3 | Dispersive phase compensation | 4 |
| 2 | Fabrication of metasurface samples | 6 |
| 2.1 | Phase and Transmission maps | 8 |
| 3 | Fourier space imaging microscopy | 9 |
| 3.1 | Setup | 9 |
| 3.2 | Dispersion of metasurface samples | 10 |
| 3.3 | Dispersion of prism | 13 |
| 4 | Achromatic prism analytical approach | 14 |
| 4.1 | Analytical results | 19 |
| 5 | Achieving Dispersion Compensation | 20 |
| 6 | Conclusion for Dispersion Compensation | 26 |

| | | |
|-----|---|----|
| 7 | Ellipsometry | 28 |
| 7.1 | Dispersion curves of ZnO thin films by ellipsometry | 29 |
| 8 | Broadband achromatic metalens | 31 |
| 9 | Appendix | 32 |
| | BIBLIOGRAPHY | 34 |

List of figures

| | |
|---|----|
| 1.1 Wavefront shaping with the use of metasurfaces [21] | 1 |
| 1.2 Anomalous refraction of light | 1 |
| 1.3 Bulk vs flat optics | 2 |
| 1.4 Demonstrated photonic devices using flat optics | 2 |
| 1.5 Spherical and coma aberrations corrected with aplanatic lens. | 3 |
| 1.6 Focussing problem with different wavelengths operating on a lens | 3 |
| 1.7 Prism turning achromatic with the use of metasurfaces | 5 |
| 2.1 Fabrication steps for TiO ₂ metasurfaces | 6 |
| 2.2 Schematic of different phase gradient samples, SEM images | 7 |
| 2.3 Phase and transmission maps | 8 |
| 3.1 Fourier microscopy setup | 9 |
| 3.2 Alignment for metasurfaces dispersion measurement | 10 |
| 3.3 Metasurface dispersion in k-space sample A | 11 |
| 3.4 Metasurface dispersion in k-space sample B | 12 |
| 3.5 Metasurface dispersion in k-space sample C | 12 |
| 3.6 Metasurface dispersion in k-space sample A | 13 |
| 3.7 Prism dispersion alignment and k space measurement for 500-800 nm | 13 |

| | | |
|-----|--|----|
| 4.1 | Opposite dispersion trend of metasurface phase gradient and prism | 14 |
| 4.2 | Schematic of light refraction through prism with phase gradient at interface | 15 |
| 4.3 | Plot of dispersion as a function of wavelength for glass | 19 |
| 4.4 | Constant deviation angle in metasurfaces coupled prism | 19 |
| 4.5 | Schematic of ray optics in achromatic prism | 19 |
| 5.1 | Prism dispersion and compensated prism dispersion | 20 |
| 5.2 | Compensated prism dispersion in 500-600 nm with three different gradients | 21 |
| 5.3 | Comparative plot of compensated dispersion in 500-600 nm | 22 |
| 5.4 | Comparative plot of compensated dispersion in 600-700 nm | 23 |
| 5.5 | Comparative plot of compensated dispersion in 500-600 nm | 24 |
| 7.1 | Ellipsometry setup schematic | 29 |
| 7.2 | Ellipsometry measurements for Ga doped ZnO thin films | 30 |

Chapter 1

Introduction

1.1 Metasurfaces and flat optics

Optical components shape the wavefront of light by relying on the gradual phase changes accumulated along the path [22]. Metamaterials exhibit the ability to bend light in peculiar ways [1, 2] giving rise to novel phenomena of negative refraction, subwavelength-imaging and cloaking [3, 4]. Introduction of abrupt phase shift along the optical path and over the scale of the wavelength allows light propagation to have new degrees of freedom and this propagation is consistent with the Fermat's principle. Optical resonators in the configuration of 2D array having subwavelength separation and phase response which changes spatially can imprint such phase discontinuities when light traverses the interface between two media while propagation [5]. Plasmonic antennas are a popular choice of resonators [6, 7] which bring about phase discontinuity at interfaces thereby tailoring the wavefront at will. Such molding of optical space due to modification in phase, amplitude and polarization gives rise to anomalous reflection and refraction which enables greater flexibility in the design of light beams and development of novel photonic devices.

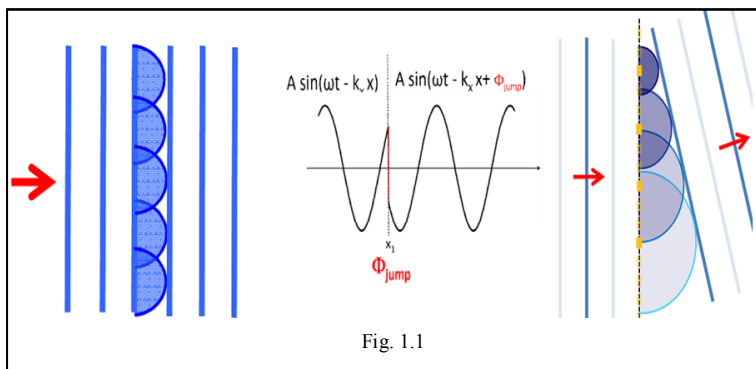


Fig. 1.1

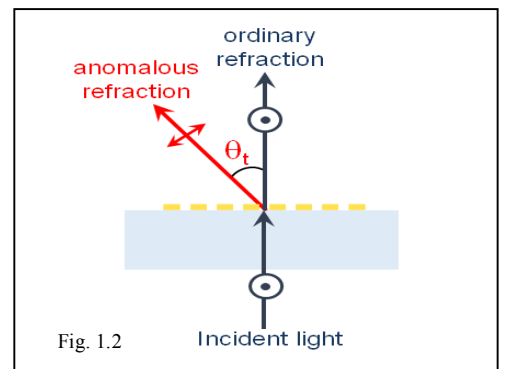


Fig. 1.2

- a. Huygen's construction of wavefronts giving secondary wavelets
- b. Desired wavefront by introduction of phase shifts, dubbed Huygen's metasurfaces [21]

Metasurfaces provide a continuous phase profile (from 0 to 2π) only with two levels of thickness (binary structure) which helps reduce the size and weight and provides ease in fabrication of diffractive planar optical components [8]. This aspect enables us to obtain ultra compact optical components and hence is ideal for designing miniaturized devices thereby allowing advancement in the field of flat optics. Flat optical devices such as blazed gratings [9-11], lenses [12-14], holographic plates [15], polarizers and waveplates have been demonstrated using different types of resonators. Metasurface coupled optical components can exhibit several functionalities, in our case, such devices rule out chromatic aberration in optical components making them function independent of wavelength.

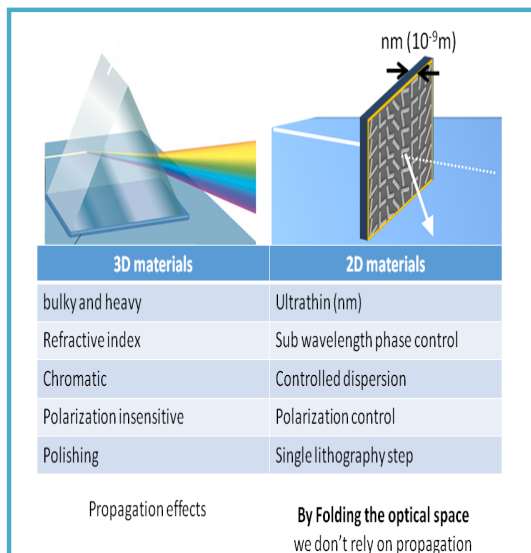


Fig. 1.3 Advantages of flat optics over bulky optics

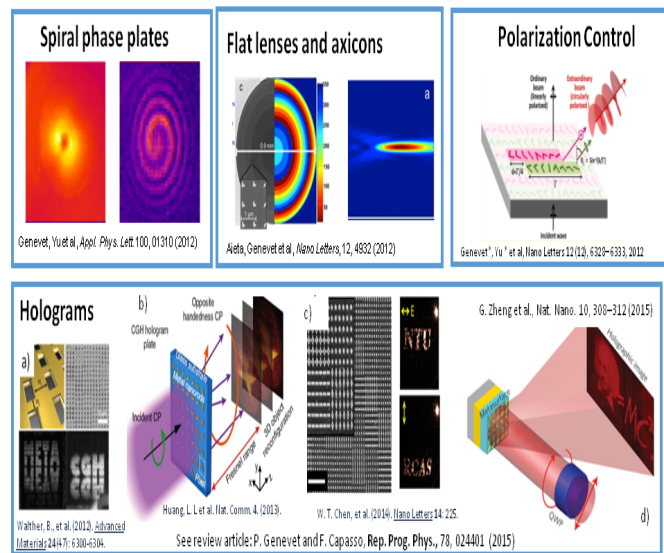


Fig. 1.4 Photonic devices using plasmonic metasurfaces and phase discontinuities tuning light properties [24, 12, 25, 26]

1.2 Problem of chromatic aberration

Optical components suffer from geometric and chromatic aberrations. Geometric aberrations arise due to distortion of monochromatic light because of the geometry of optical components and light propagation whereas chromatic aberrations have unintended separation of different colours. Such aberrations result in bad focussing of light and give poor image quality. Monochromatic spherical and coma aberrations were shown to have been corrected with the use of aplanatic metasurfaces lens in [15].

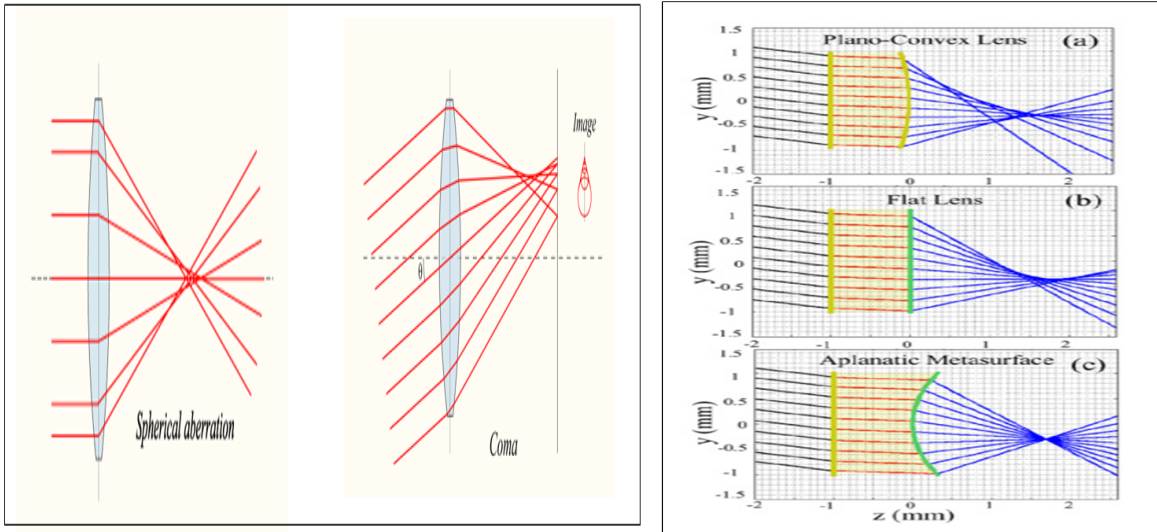
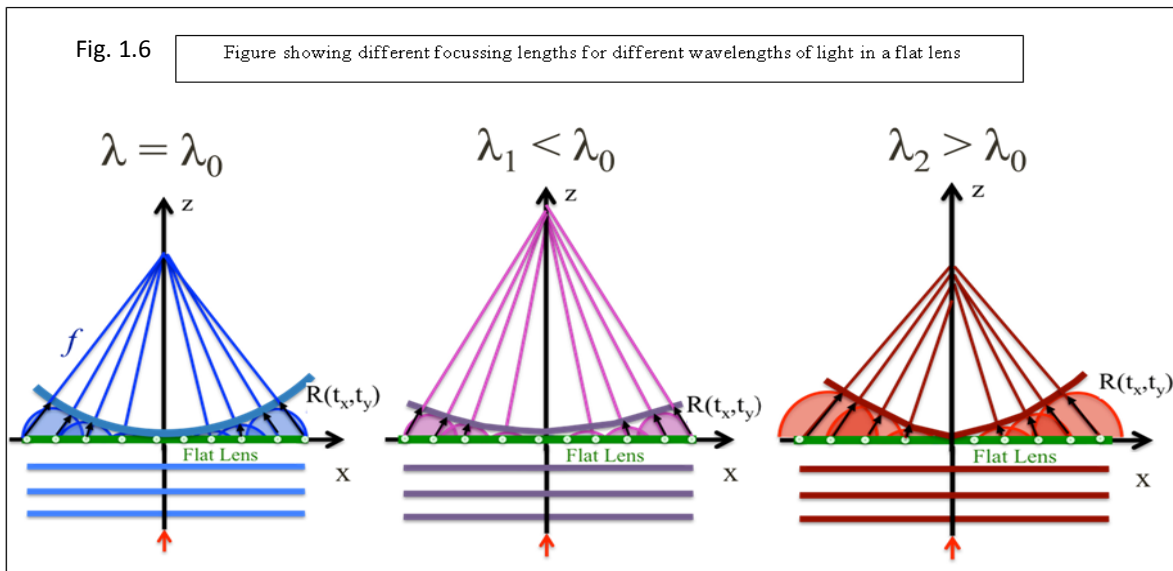


Fig. 1.5 Monochromatic spherical and coma aberrations were shown to have been corrected with the use of aplanatic metasurfaces lens.

But chromatic aberrations in flat lens still need to be corrected. Because the radius of spherical wavelength in a function of wavelength, a change in wavelength will cause change in the focal length and this way different wavelengths are focussed at different points on the optical axis giving chromatically aberrated images for a multichromatic light source.



$$R(t_x, t_y) = \frac{\lambda}{2\pi} \varphi(t_x, t_y)$$

1.3 Dispersive Phase Compensation

There has been work done to show that achromatic behaviour in metasurfaces can be exhibited if we take into account the *dispersive phase compensation*. To achieve a desired functionality, there should be constructive interference between several light paths separating the interface and the desired wavefront. Two phase terms contribute to the total accumulated phase, first term being the phase shift transmitted at a point r by the metasurfaces: ϕ_m and second term being the phase accumulated when light propagates through space: ϕ_p . Total accumulated phase is therefore:

$\phi_{tot}(r,\lambda) = \phi_m(r,\lambda) + \phi_p(r,\lambda)$. We note that $\phi_m(r,\lambda) = (-2\pi/\lambda)*l(r)$ where $l(r)$ indicates the function of the device, for example, if it is a beam deflector or a lens. For observing achromatic behaviour of the photonic system, we have to keep ϕ_{tot} constant by making sure constructive interference condition is preserved at different wavelengths. We need to design the dispersion of ϕ_m in such a way that it compensates for the wavelength dependence of ϕ_p .

Therefore, $\phi_m = -\phi_p$ [8, 23]. This equation is important for the design of achromatic metasurfaces. In this way, the dispersive phase compensation approach of flat optics highlights the advantages of diffractive optics by achieving achromatic behaviour at selected wavelengths.

In order to tackle the problem of chromatic aberrations, we need to control the change in phase, that is, dispersion, so that the function involving wavelength and phase should remain constant.

$$\lambda * \phi(x,y) = \text{constant} \quad (1)$$

The use of metasurfaces while designing optical components will thus prove beneficial as metasurfaces will control the phase at material interface for different wavelengths giving achromatic response [16]. This approach has been used to achieve achromatic response at a few selected wavelengths in the IR region, see [8]. Achromatic response was also achieved for a 60 nm bandwidth, 490-550 nm, in the visible range, see [17]. Because the previous studies covered smaller bandwidth, this study specifically aims to use the *dispersive phase compensation* mechanism to achieve achromatic response for a larger bandwidth in the visible range of 500-800 nm.

We start by taking a simple optical dispersive component, a prism. If the deviation angle for different wavelengths of light emerging out of the prism is kept constant, it would result in compensating for the dispersion. A phase gradient created by metasurfaces on the interface of prism will control the light ray to deviate with constant angle for the desired wavelengths. For this, we need to work in the wavelengths range where the dispersion of the material is linear so that the phase shifts introduced by metasurfaces having a linear gradient will refract light at angles defined by the user. We recall that the total phase accumulated by light during propagation is given by: $\phi_{tot}(r,\lambda) = \phi_m(r,\lambda) + \phi_p(r,\lambda)$. In order to have achromatic response, $\phi_{tot}(r,\lambda)$ should remain constant. Therefore, $\phi_m = -\phi_p$. Meaning, dispersion of metasurfaces will compensate for the dispersion of prism if the phase response of metasurfaces is aligned opposite to the phase response of prism on the interface.

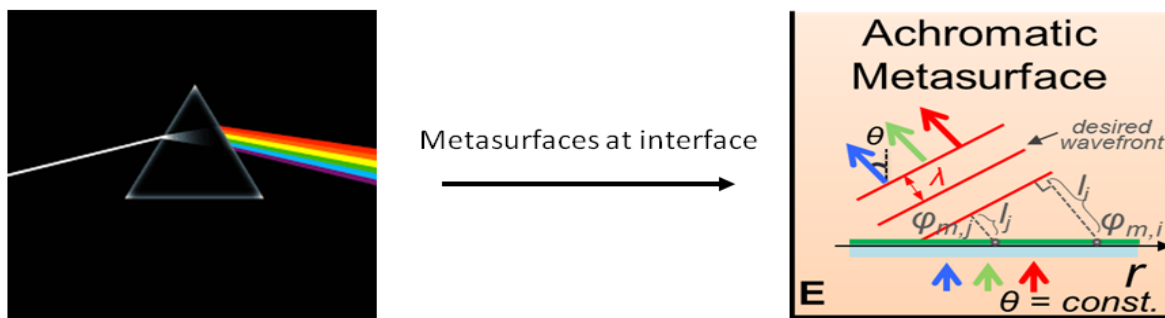


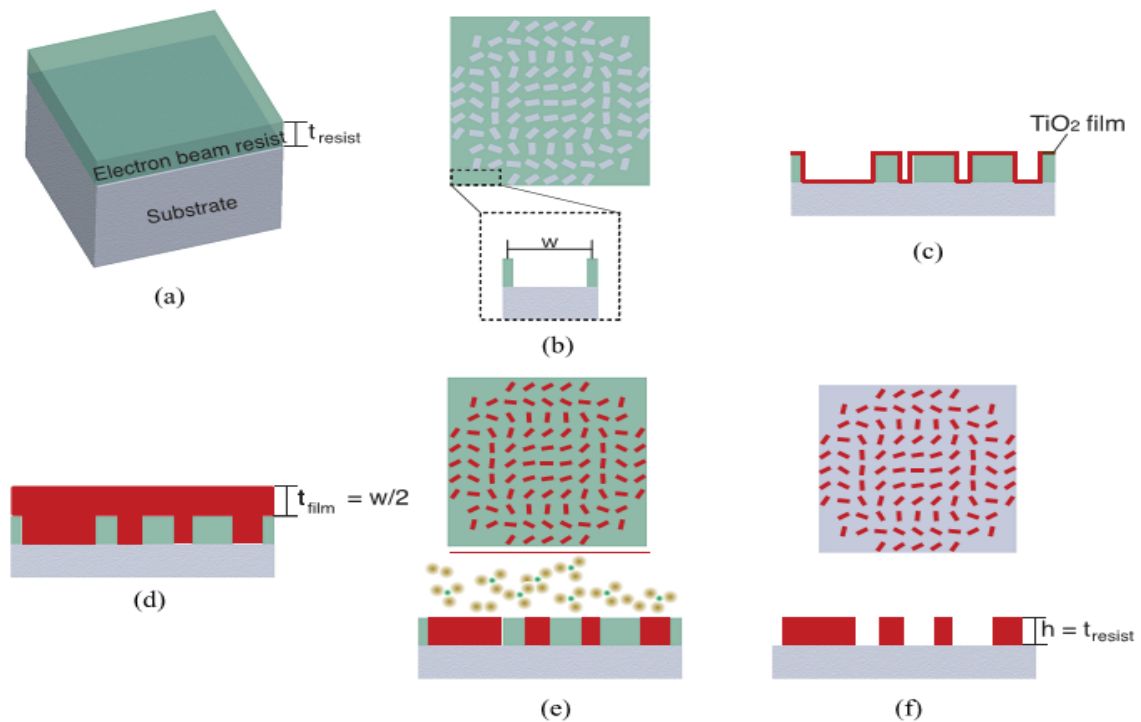
Fig. 1.7 Prism turning achromatic upon introduction of metasurfaces at prism interface

Chapter 2

Fabrication of metasurface samples

Metasurface samples made of Titanium dioxide on glass substrate having different phase gradient value were fabricated and provided by the Capasso group at Harvard. We choose nanopillar metasurface geometry for our metasurfaces working in the visible range of 500-800 nm. The nanopillar geometry is polarization insensitive and we need not worry about change in polarization when we do imaging business in the Fourier space for our dispersion measurement study [19].

Fig. 2.1 Fabrication steps for TiO_2 metasurface sample



Step a- Spin coat a glass substrate with Electron Beam Lithography using resist (ZEP 520 A)

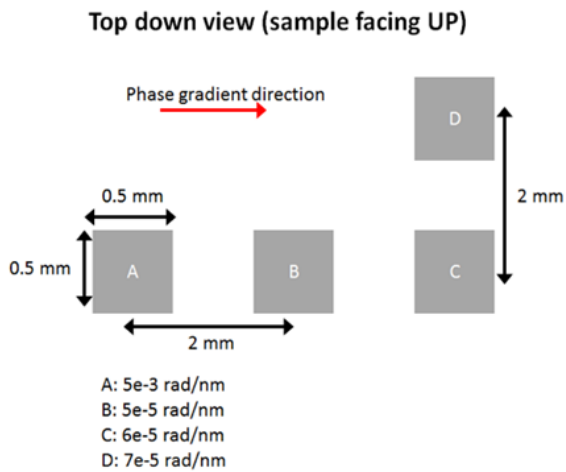
Step b- Expose the resist by EBL and further develop it in 99% o-xylene.

Step c- Start Atomic Layer Deposition of TiO_2 onto the patterned resist

Step d- Continue ALD of TiO_2 upto the required thickness on top of the resist

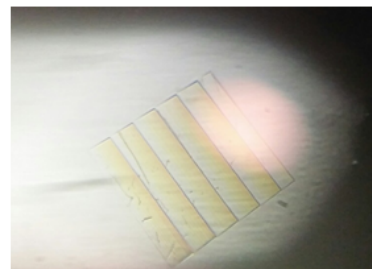
Step e- TiO_2 layer is formed above the resist as a result of conformal deposition of ALD, we now have to etch down the TiO_2 till we just touch the resist layer.

Step f- Resist is removed by using PB bath which works overnight to get rid of resist. Finally we get nanostructures of same height as that of spin-coated resist



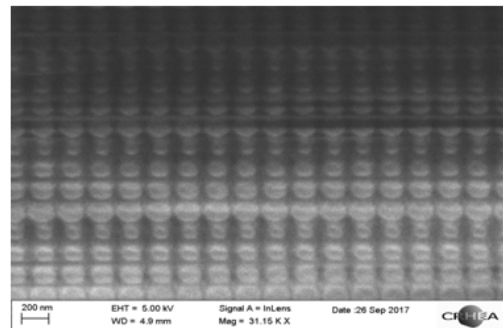
Schematic showing four metasurfaces samples with different phase gradients

Fig. 2.2 Fabricated metasurface nanopillar samples

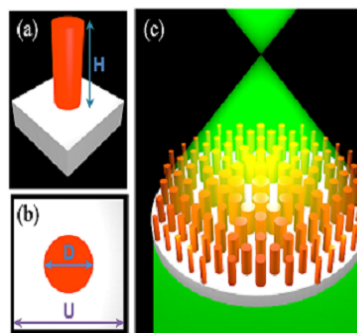


Sample D as observed under an optical microscope

Each square has a periodic nanopillar assembly of metasurfaces



SEM image of sample A



Metasurface assembly made up of nanopillars with different diameter D and height H

2.1 Phase and Transmission maps

To tailor the wavefront like the one shown in figure 10, we need to have a constant phase gradient and equal amplitude condition along the interface on x-axis. A change in the phase shift between the emitted and incident radiation occurs for an optical resonator across resonance. It is therefore possible to tailor the geometry of resonators present in an array and hence the frequency response along x-axis so that every element imparts the required phase shift to engineer the wavefront as desired [5]. We run FDTD simulations to evaluate the phase response of electromagnetic waves by varying geometric parameters such as diameter, height of metasurface nanopillar elements in the array across the bandwidth of interest. Given below are the phase and transmission maps of simulations carried out for TiO₂ nanopillar metasurface assembly. The phase map has varying diameter on x-axis, varying wavelength on y-axis and the colour bar shows phase shifts covering the 0 to 2π range needed to provide full control of wavelength. Similarly, transmission efficiency becomes important for optical resonators involving transmitted light applications. The colour bar shows 0 as minimum transmission and 1 as maximum transmission exhibited by elements at the required wavelengths for different diameters. To achieve achromaticity, it is required that the element at a point r on x-axis imparts the same phase shift for all wavelengths of interest. Every such element on x-axis after imparting the required phase shift at that point will together work to give a constant phase gradient and shape the wavefront.

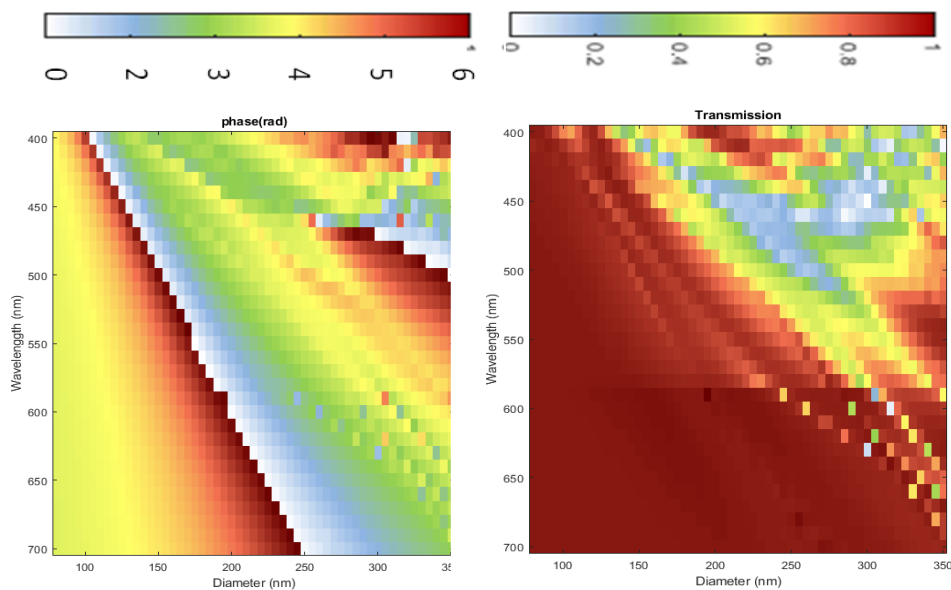


Fig. 2.3 Tailored wavefront and phase and transmission maps

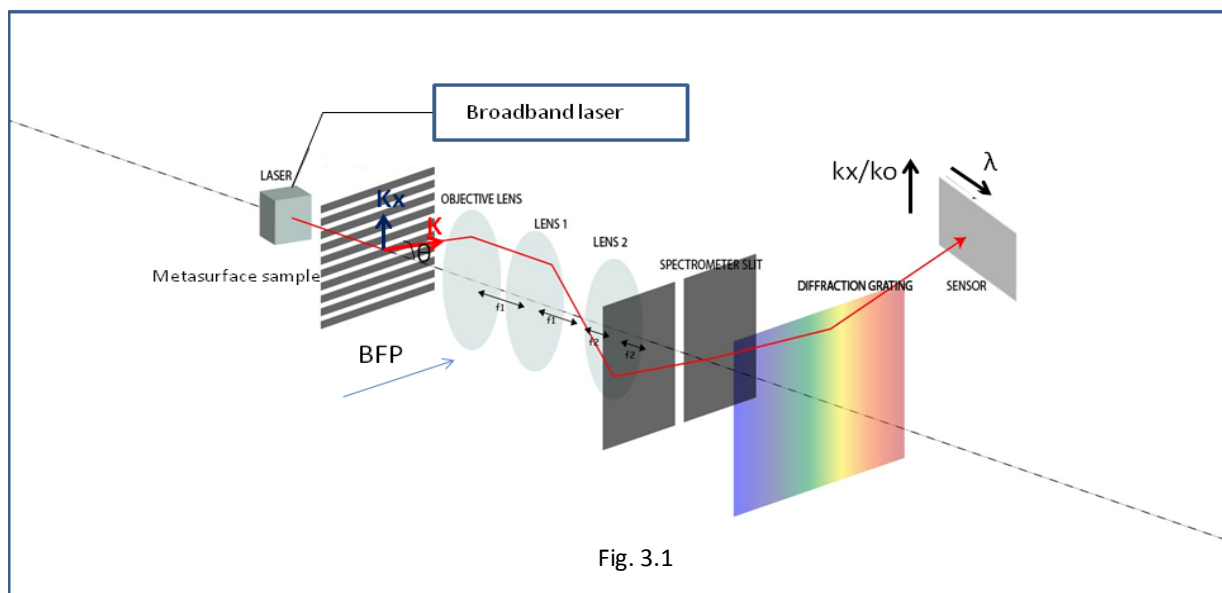
Chapter 3

Fourier space imaging microscopy

3.1 Setup

In order to measure dispersion of our metasurface samples and prism, we use Fourier plane imaging microscopy [20]. This technique will give us k space information of our light vector transmitting through the material in the Fourier space thereby giving us angle resolved information of dispersion of materials.

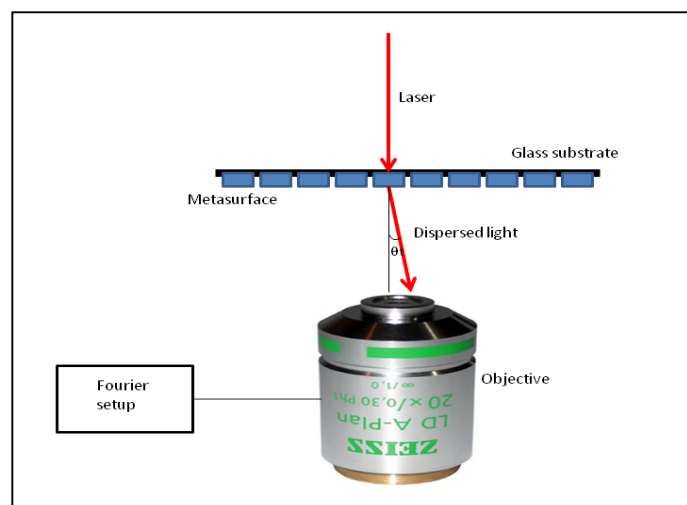
Dispersion measurement- **Fourier plane Microscopy**



The above Fourier setup is used to measure dispersion of materials. We have a supercontinuum laser source giving a broadband light carried by a fiber. The laser is shone on the metasurface sample and the refracted light will now enter the objective of an optical microscope. The microscope objective will do a Fourier transform of the refracted light coming from different angles and image it on the back focal plane (BFP) of the microscope objective. Thus, rays coming from different angles will form distinct points in the k_x - k_y space on the BFP of the microscope objective. Therefore, we say that the BFP holds the k -space information. Now, we do not want to see only the k_x - k_y information of our light vector, but we want to see it as a function of wavelength. We therefore relay this BFP image using lens1 and lens2 to get it into a spectrometer. The diffraction grating of the spectrometer will give us the wavelengths information. Our sensor is a two-dimensional CCD camera. Because we have the wavelength information on one axis, we are left with only one another axis to project the k -space information. We align the metasurface sample in such a way that the k_x information will be projected on the axis orthogonal to the wavelength axis. This way, we see the k_x information as a function of wavelengths on the computer screen.

3.2 Dispersion of metasurface samples

Dispersion measurements were performed on four metasurface samples having different phase gradient value by shining laser at normal incidence and seeing the dispersed light projected on the detector through a Fourier setup. Fig. 4.3 showing alignment to measure sample dispersion.



Sample A: phase gradient = $5 \cdot 10^{-3}$ rad/nm, imaged with 20x microscope objective

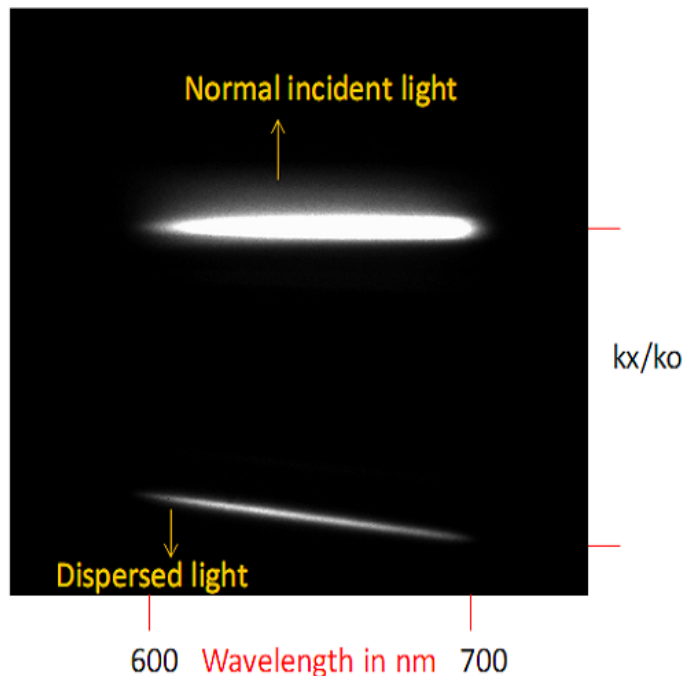


Fig. 3.3 showing dispersion of metasurface in k-space

This is the dispersion image we obtain in the k-space. The wavelength information is on x-axis and kx/k_0 information on y-axis. The slope zero line is the light coming straight through the sample when shone with normal incidence. The line having a slope is actually the dispersed light. We understand that for one particular wavelength the number of pixels counted from the normal incident light to the dispersed light gives us a measure of light getting deflected from the normal, which is $\sin\theta$. And this $\sin\theta$ increases linearly with the wavelength. This way we indeed are seeing the linear dispersion of metasurfaces in k-space.

This can be supported by the generalized refraction law at the metasurface-air interface:

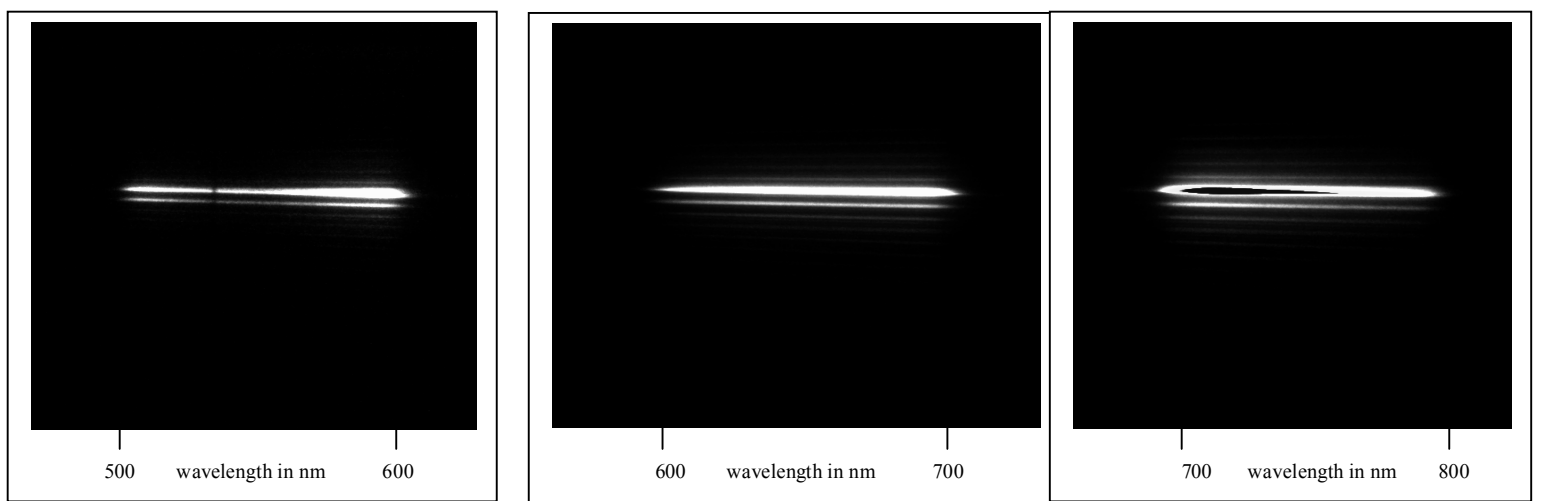
$$n_1 \sin\theta_t - n_2 \sin\theta_i = \left(\frac{\lambda}{2\pi}\right) \left(\frac{d\phi}{dx}\right)$$

As $\theta_i = 0$ and $n_1 = 1$, we get:

$$\sin\theta_t = \left(\frac{\lambda}{2\pi}\right) \left(\frac{d\phi}{dx}\right)$$

We here see that $\sin\theta_t$ increases linearly with λ for a constant phase gradient value.

Fig. 3.4 **Sample B**: phase gradient = $5 \cdot 10^{-5}$ rad/ nm, imaged with 4x microscope objective



Sample B has the least phase gradient value. This being a very shallow phase gradient, the dispersion on the y-axis, that is, the k_x/k_0 value is very less. The $n=0$ order (upper line) is for the light passing straight through the sample when illuminated with normal incidence. $n=1$ order (lower line) is the dispersed light. Measurements were taken for wavelength range 500-800 nm. Lines are saturated at the ends because of focussing problems and misalignments.

Fig. 3.5 **Sample C**: phase gradient = $6 \cdot 10^{-5}$ rad/nm, imaged with 4x microscope objective

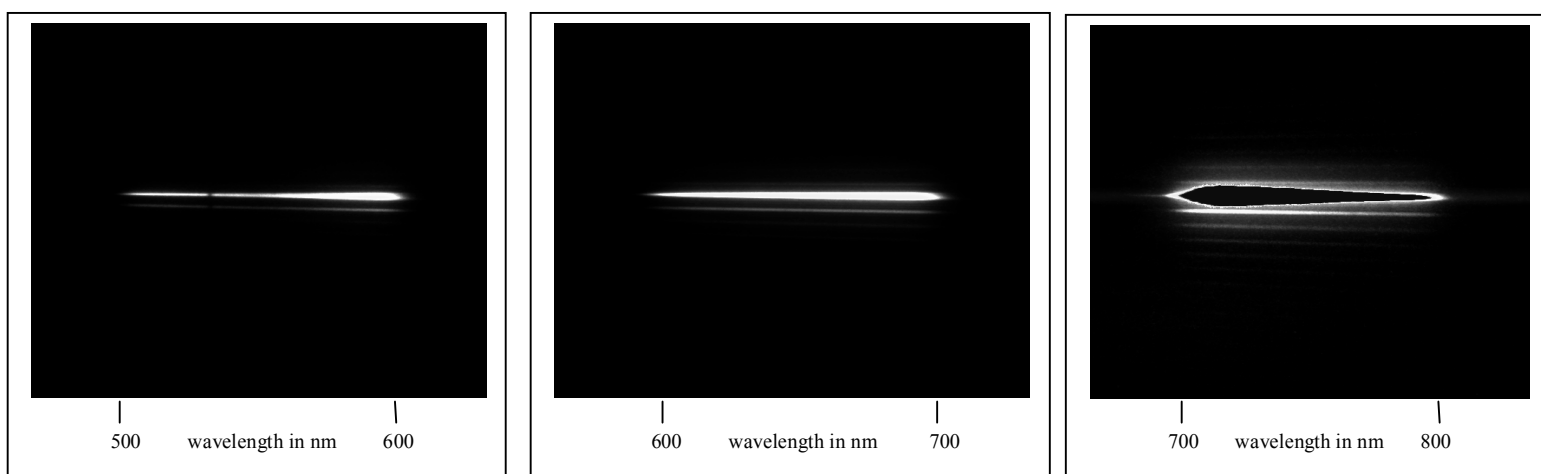
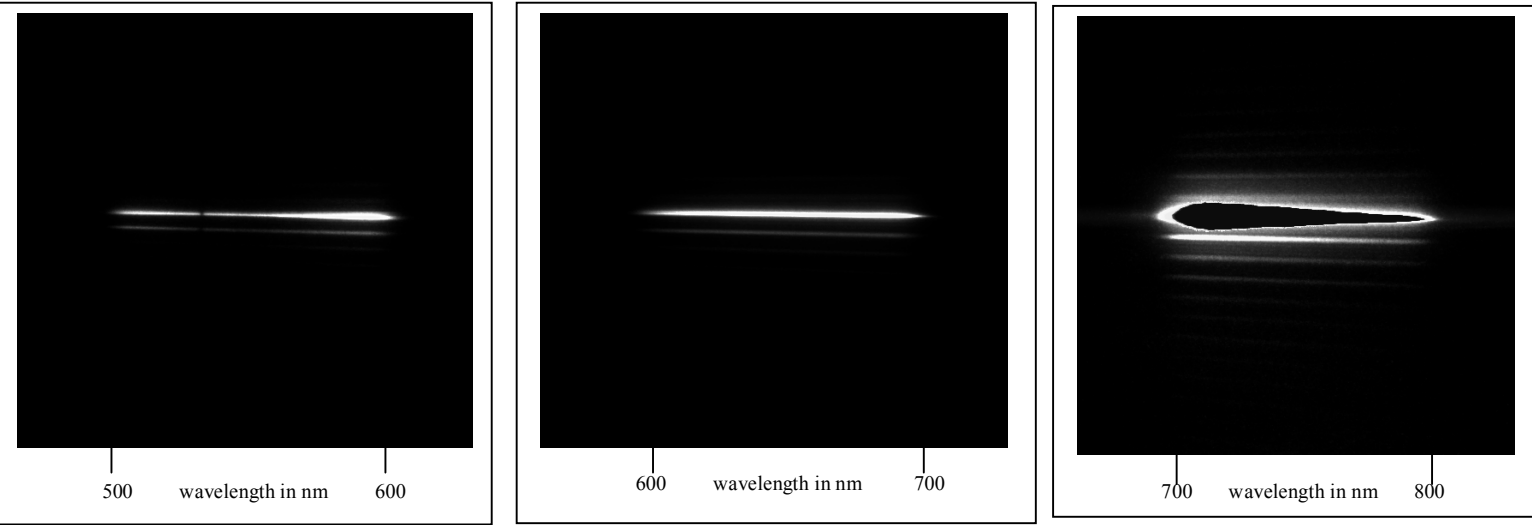
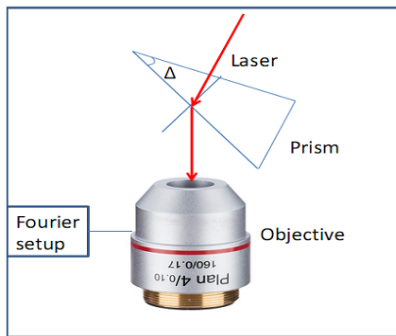


Fig. 3.6 **Sample D**: phase gradient = $7 \cdot 10^{-5}$ rad/nm, imaged with 4x microscope objective

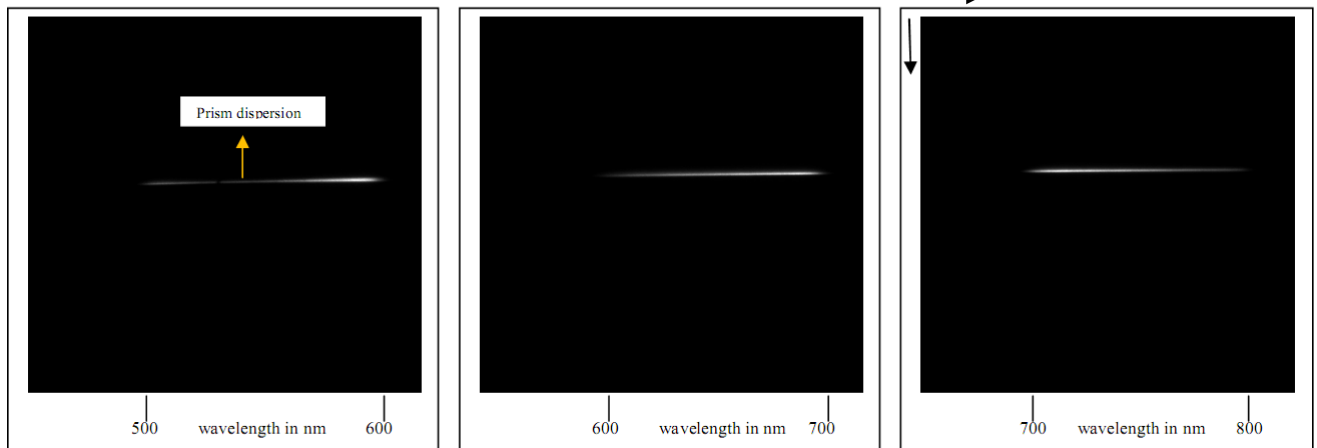


3.3 Dispersion of prism

Fig. 3.7 **Prism dispersion**: imaged with 4x microscope objective



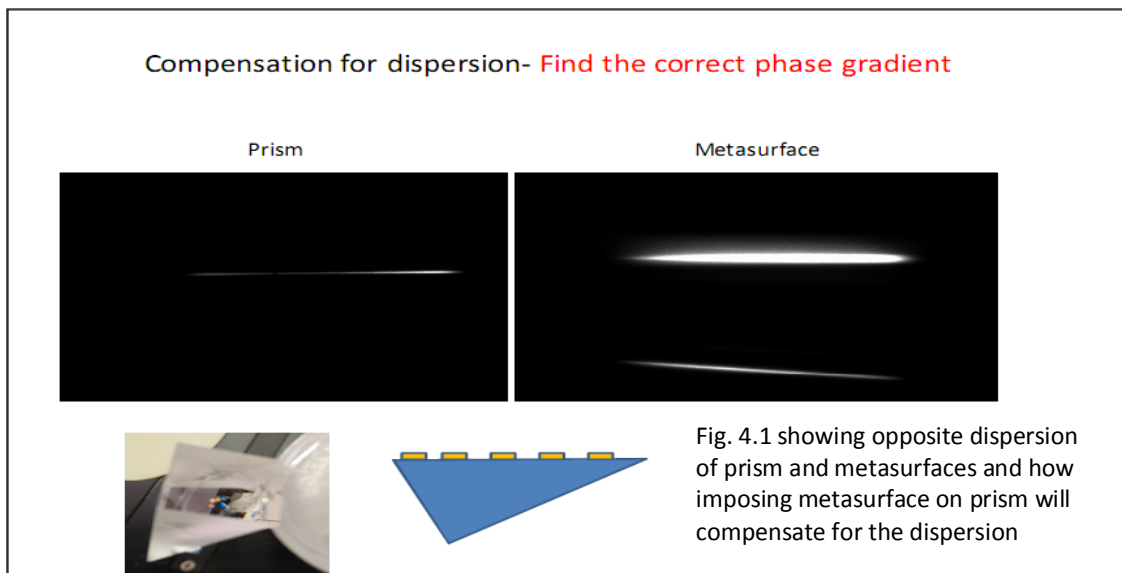
Shown on the left is a schematic for the measuring the dispersion of the prism. The prism of prism angle $\Delta = 30$ degree is illuminated with normal incident light. The prism needs to be mounted with some tilt so that the refracted light can enter the microscope objective. Otherwise, low numerical aperture of the objective may not be able to collect all the refracted light.



Chapter 4

Achromatic prism analytical approach

The prism dispersion measurements in Fig. 16 show a linear dispersion of prism in wavelength range 500-800 nm. The dispersion is actually pretty less as the slope is very small. So in order to compensate for its dispersion we need a very shallow phase gradient to be applied on the interface. Because the pixel coordinate for the image starts at the top left hand corner at (0, 0) and increases towards right for x-axis and down for y-axis, the prism dispersion slope is negative here; whereas the metasurface dispersion slope is positive. We indeed need this opposite phase response between the prism and metasurface to achieve achromatic behaviour as $\phi_m = -\phi_p$. All we need to do is find the correct phase gradient sample, align it on the prism interface and look for compensation of prism dispersion.



Calculating the required phase gradient:

The aim is to design a prism which when incident with light shows achromatic behaviour for different wavelengths of light. To achieve this, we set the deviation angle for different wavelengths to be constant. Normal prisms show dispersion phenomenon for light. But in order to compensate for the dispersion and achieve constant deviation angle for all wavelengths, we use a metasurface to create a phase gradient along interfaces. This would mold the light ray in such a way that it deviates with a constant angle for the desired number of wavelengths.

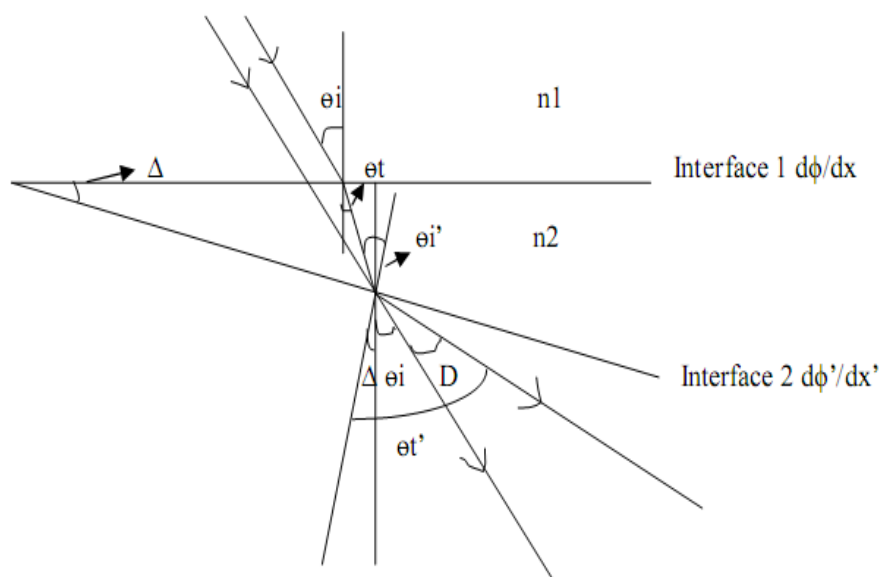


Fig. 4.2 Schematic of refraction of light through two prism faces with some phase

Figure 1 describes the path of incident light and it getting refracted from the two interfaces of a prism. The prism angle is Δ . Interface 1 and interface 2 may be embedded with a metasurface to establish a phase gradient ($d\phi/dx$) along interface 1 and ($d\phi'/dx'$) along interface 2. The incident light comes at an angle θ_i on interface 1. The ray is then refracted in the prism with angle θ_t . The refracted ray is again incident on interface 2 with an angle $\theta_{i'}$. The final transmitted ray comes out of the prism with an angle $\theta_{t'}$. The angle between the incident ray and the final transmitted ray is called the deviation angle D . The refractive index of the material of prism is n_2 and that of air is $n_1=1$.

In order to achieve same deviation angle condition for all wavelengths, a theoretical construct with the governing equations is provided here.

Refraction at interface 1 is given by the expression:

$$n_2 \sin \theta_t - n_1 \sin \theta_i = \left(\frac{\lambda}{2\pi} \right) \left(\frac{d\phi}{dx} \right) \quad (1)$$

Refraction at interface 2 is given by the expression:

$$n_1 \sin \theta_t' - n_2 \sin \theta_i' = \left(\frac{\lambda}{2\pi} \right) \left(\frac{d\phi'}{dx'} \right) \quad (2)$$

By geometry,

$$\theta_i' = \theta_t + \Delta \quad (3)$$

$$D = \theta_t' - (\Delta + \theta_i) \quad (4)$$

Equation (4) can be written as,

$$D = \theta_t' - \Delta - \theta_i \quad (5)$$

Now using equation (2) expression for θ_t' becomes:

$$\theta_t' = \arcsin \left[\left(\frac{\lambda}{2\pi n_1} \right) \left(\frac{d\phi'}{dx'} \right) + \left(\frac{n_2}{n_1} \right) \sin \theta_i' \right] \quad (6)$$

But $\theta_i' = \theta_t + \Delta$, therefore $\sin \theta_i' = \sin(\theta_t + \Delta) = \sin \theta_t \cos \Delta + \cos \theta_t \sin \Delta$

Now equation (6) becomes:

$$\theta_t' = \arcsin \left[\left(\frac{\lambda}{2\pi n_1} \right) \left(\frac{d\phi'}{dx'} \right) + \left(\frac{n_2}{n_1} \right) (\sin \theta_t \cos \Delta + \cos \theta_t \sin \Delta) \right] \quad (7)$$

From equation (1) we get the expression for $\sin \theta_t$ as:

$$\sin \theta_t = \left(\frac{\lambda}{2\pi n_2} \right) \left(\frac{d\phi}{dx} \right) + \left(\frac{n_1}{n_2} \right) \sin \theta_i \quad (8)$$

And

$$\cos \theta_t = \sqrt{1 - \left(\left(\frac{\lambda}{2\pi n_2} \right) \left(\frac{d\phi}{dx} \right) + \left(\frac{n_1}{n_2} \right) \sin \theta_i \right)^2} \quad (9)$$

Putting equations (8) and (9) in equation (7) we get,

$$\begin{aligned} \theta_t' = & \arcsin \left[\left(\frac{\lambda}{2\pi n_1} \right) \left(\frac{d\phi'}{dx'} \right) + \right. \\ & \left. \left(\frac{n_2}{n_1} \right) \left(\left(\left(\frac{\lambda}{2\pi n_2} \right) \left(\frac{d\phi}{dx} \right) + \left(\frac{n_1}{n_2} \right) \sin \theta_i \right) \cos \Delta + \sqrt{1 - \left(\left(\frac{\lambda}{2\pi n_2} \right) \left(\frac{d\phi}{dx} \right) + \left(\frac{n_1}{n_2} \right) \sin \theta_i \right)^2} \sin \Delta \right) \right] \quad (10) \end{aligned}$$

$$D = \arcsin \left[\left(\frac{\lambda}{2\pi n_1} \right) \left(\frac{d\phi'}{dx'} \right) + \left(\frac{n_2}{n_1} \right) \left(\left(\left(\frac{\lambda}{2\pi n_2} \right) \left(\frac{d\phi}{dx} \right) + \left(\frac{n_1}{n_2} \right) \sin \theta_i \right) \cos \Delta + \sqrt{1 - \left(\left(\frac{\lambda}{2\pi n_2} \right) \left(\frac{d\phi}{dx} \right) + \left(\frac{n_1}{n_2} \right) \sin \theta_i \right)^2 \sin^2 \Delta} \right) \right] \quad (11)$$

We need to keep terms linear in λ . We work in the region where $n_2 = a\lambda + b$, so we eliminate terms of the form $1/\lambda$. Therefore,

$$\left(\frac{\lambda}{2\pi n_2} \right) \left(\frac{d\phi}{dx} \right) + \left(\frac{n_1}{n_2} \right) \sin \theta_i = 0 \quad (12)$$

$$\left(\frac{\lambda}{2\pi} \right) \left(\frac{d\phi}{dx} \right) = -n_1 \sin \theta_i \quad (13)$$

If equation (13) holds, it means $\sin \theta_t = 0$; (see equation (1))

Therefore, we have $\theta_t = 0$, that is we have zero transmission angle when the incident light gets refracted from interface 1.

$$\left(\frac{d\phi}{dx} \right) = - \left(\frac{2\pi n_1 \sin \theta_i}{\lambda} \right) \quad (14)$$

For $\left(\frac{d\phi}{dx} \right)$ to be independent of wavelength, we are conditioned to set $\theta_i = 0$

$$\left(\frac{d\phi}{dx} \right) = 0, \theta_i = 0, \theta_t = 0$$

It means we have normal incidence of light at interface 1.

Using the condition given in equation (12), the modified equation (11) for D now becomes:

$$D = \arcsin \left[\left(\frac{\lambda}{2\pi n_1} \right) \left(\frac{d\phi'}{dx'} \right) + \left(\frac{n_2}{n_1} \right) (\sin \Delta) \right] - \Delta \quad (15)$$

The deviation angle D is set to be constant for all wavelengths of interest.

Also, refractive index n_2 is dependent on the wavelength. We want to work in a region where n_2 becomes a linear function of λ with 'a' as the slope and 'b' as y intercept. $n_1 = 1$.

$$n_2 = a\lambda + b \quad (16)$$

By putting equation (16) in equation (15) and rearranging the terms, we get:

$$\sin(D + \Delta) = \left(\frac{\lambda}{2\pi} \right) \left(\frac{d\phi'}{dx'} \right) + (a\lambda + b) (\sin \Delta) \quad (17)$$

Solving equation (17) further,

$$\sin(D + \Delta) - b \sin \Delta = \lambda \left[a \sin \Delta + \left(\frac{1}{2\pi} \right) \left(\frac{d\phi'}{dx'} \right) \right] \quad (18)$$

We want D to be constant even when λ can vary. It means we should set the coefficient of λ to zero on RHS of equation (18)

$$a \sin \Delta + \left(\frac{1}{2\pi}\right) \left(\frac{d\phi'}{dx'}\right) = 0 \quad (19)$$

Using equation (19), we now get the expression for $\left(\frac{d\phi'}{dx'}\right)$ as:

$$\left(\frac{d\phi'}{dx'}\right) = -2\pi a \sin \Delta \quad (20)$$

Now that the RHS of equation (18) is zero, we get the simplified expression for D as:

$$D = \arcsin(b \sin \Delta) - \Delta \quad (21)$$

Now that the theoretical construct is complete, we will use the above equations to see the behaviour of deviation angle for different wavelengths by using the data given for glass and this data was provided by Accurion.

In order to plot Deviation angle wrt wavelength, we follow further steps:

Step 1- To find the range where n_2 is linear wrt λ , we plot $dn/d\lambda$ vs λ and find the range for λ where $dn/d\lambda$ is constant.

Step 2- We then plot n vs λ , only by taking the range for λ where n_2 is linear wrt λ .

Step 3- The plot should give us a linear trend. By doing a linear fit, we get the line equation and constants (slope= a, y intercept= b)

Step 4- We put the parameters like the expression for $d\phi'/dx'$ from equation (20) and set the prism angle Δ to some value in equation (15)

Step 5- Now we plot D as a function of λ by using equation (15), value of n_2 will correspond to that particular λ from the available data.

Step 6- On plotting D vs λ , we see a region where D remains constant while λ varies. The range is the same in which we find n_2 to have a linear trend wrt λ .

In this way, we are able to get a constant deviation angle for different colours of light thus achieving the achromatic behaviour for a prism by introducing the phase gradient along interfaces.

Analytical Results:

1. Plot of refractive index vs wavelength for glass

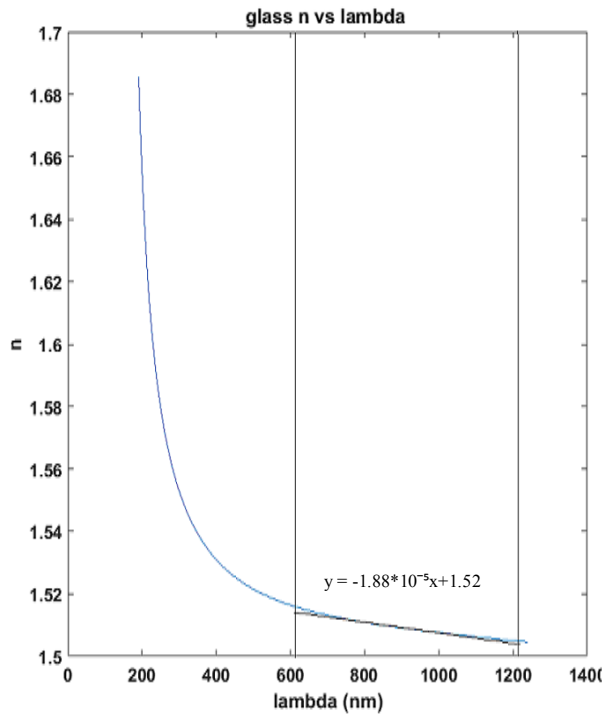


Fig. 4.3 Refractive index of glass varies with wavelength. We work in the linear dispersion regime to satisfy dispersion compensation property. The linear dispersion is observed from 600-1000 nm. The slope of this dispersion is important to determine the phase gradient to be imposed on prism interface with prism angle Δ , see equation 20. In this way, for a prism angle of 30° , calculated value of phase gradient is $6 \cdot 10^{-5}$ rad/nm. A phase gradient of this order will help compensating for the dispersion of prism.

2. Plot of deviation angle vs wavelength

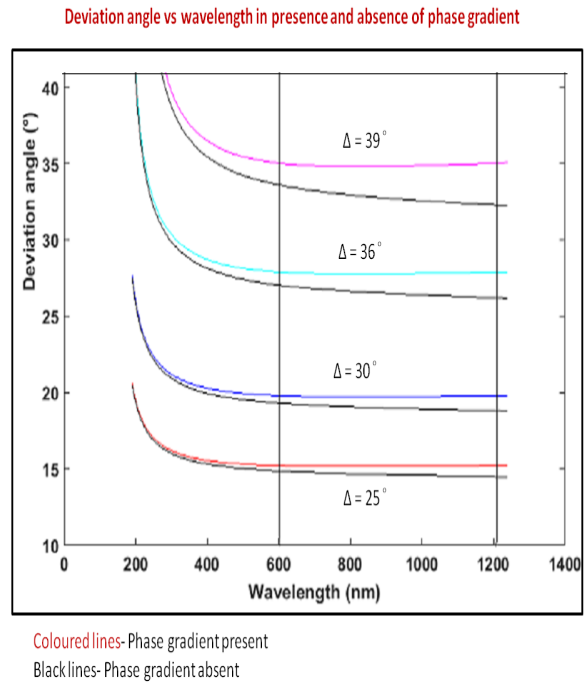
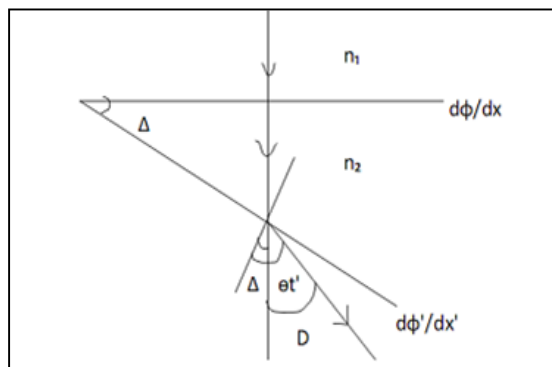


Fig. 4.4 This deviation angle vs wavelength plot shows that when a phase gradient is applied on prism interface, the dispersion is compensated, meaning, the deviation angle D now becomes constant for wavelengths in which material has linear dispersion. If a phase gradient is not applied, then the prism exhibits normal dispersion behaviour with varying deviation angle as the wavelength increases.

Fig. 4.5 Schematic of prism being achromatic, having constant deviation angle D for all wavelengths of interest when illuminated with normal incidence



Chapter 5

Achieving Dispersion Compensation

When we say we want to compensate for material dispersion, in this case, for the prism, we expect a k-space image where the refracted light has slope zero across the continuous wavelength range. Therefore, the slope of such a compensated dispersed light should resemble the slope of normal incident light. The normal incident light is going to propagate through free space without encountering any dispersive material and straightaway going into the microscope objective. The result is a slope zero line in the k_x/k_0 vs wavelength image where there is no dispersion.

Below is an image on the left with a free space propagated normal incident light showing no dispersion and on the right is the compensated dispersion of prism when a correct phase gradient is applied on its interface.

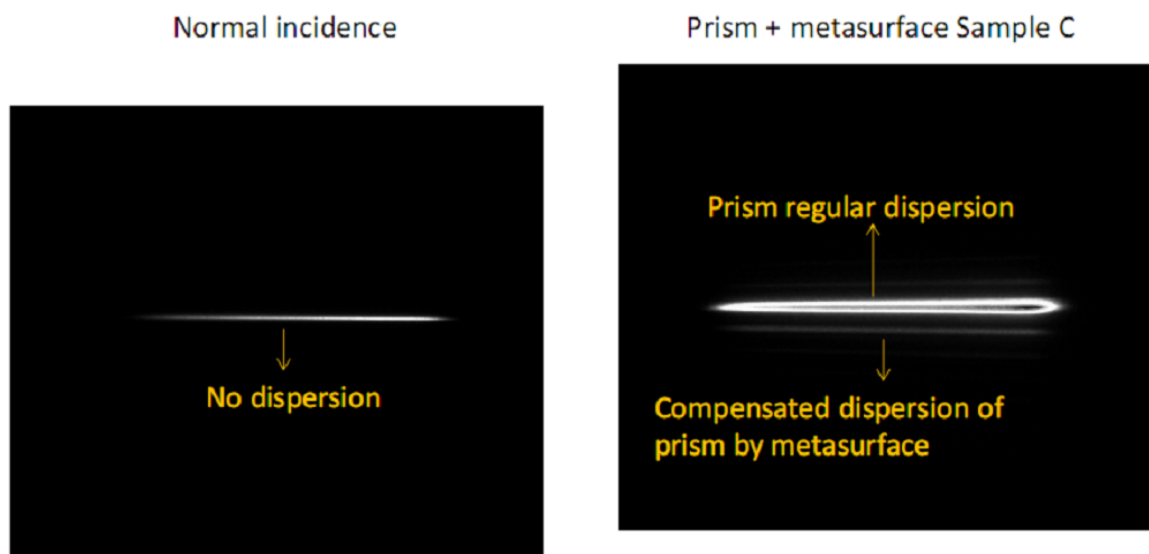
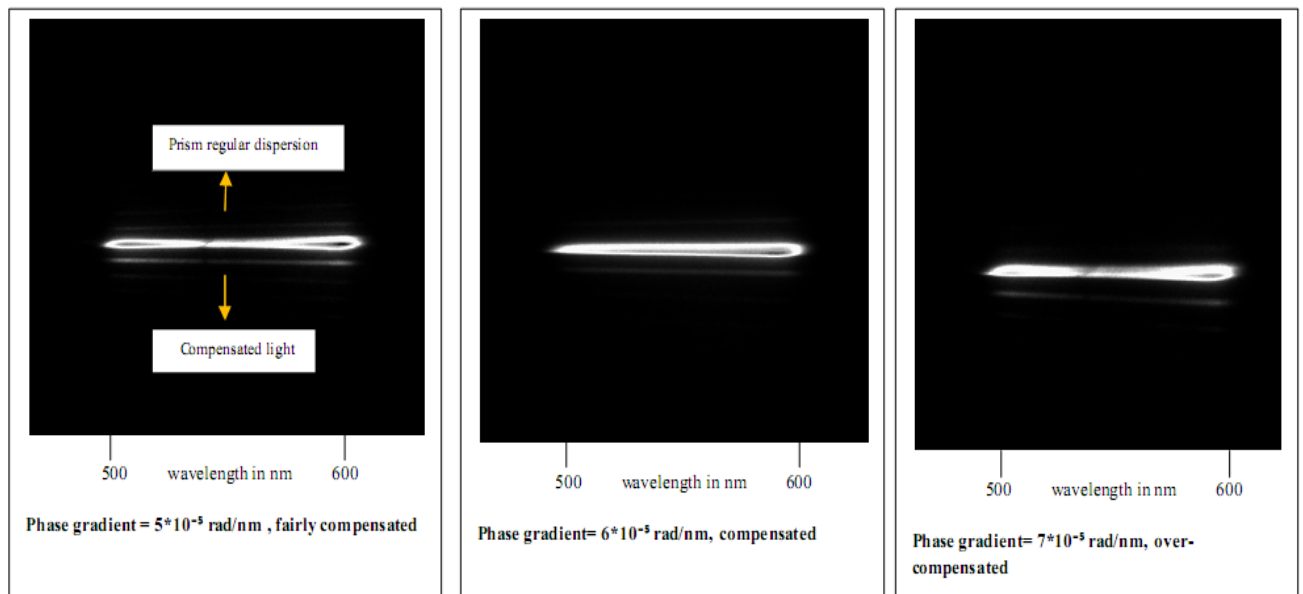


Fig. 5.1 Compensated dispersion in prism

In the image on the right, we have a prism with a phase gradient of 6×10^{-5} rad/nm applied on its interface. Lines are a bit saturated because of focussing problems. The dispersion measurement shows the regular dispersion of prism (positive slope) in the upper line. This may be because the metasurfaces may not be able to deflect whole of the incident light to a user-defined angle. The lower line has a slope smaller than the regular dispersion. We thus say that the phase gradient has helped compensate for the dispersion of prism. Now the slope of lower line in ideal case should resemble the slope of normal incident light on the right to show achromatic response of the prism across the given range of wavelengths.

Fig. 5.2 Dispersion compensation by phase gradient 5×10^{-5} rad/nm, 6×10^{-5} rad/nm and 7×10^{-5} rad/nm in wavelength range 500-600 nm



-Dispersion compensation results for 500-600 nm

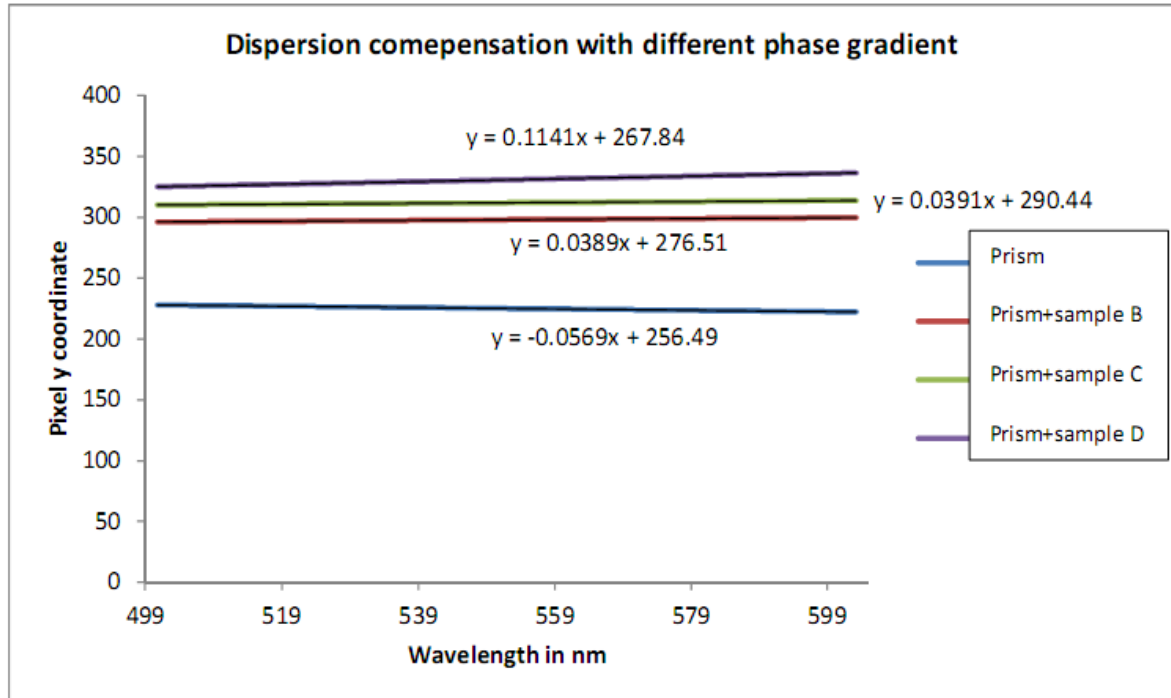


Fig. 5.3 In this graph we plot the compensated dispersion lines of a prism which has metasurface samples on its interface. Compensated dispersion lines are plotted taking different phase gradient values in the range 500-600 nm. The blue line shows prism regular dispersion having a negative slope. An ideally compensated light should have a zero slope so that the deflection angle is constant for all wavelengths. Prism dispersion compensated with sample B of 5×10^{-5} rad/nm phase gradient gives us a slope of 0.0389 which is the best compensation achieved in 500-600 nm bandwidth. Prism dispersion compensated with sample C of 6×10^{-5} rad/nm phase gradient gives us a slope of 0.039 which is compensating similarly when compared to 5×10^{-5} rad/nm phase gradient. Prism dispersion is over-compensated by sample D of 7×10^{-5} rad/nm phase gradient with a slope of 0.1141.

-Dispersion compensation results for 600-700 nm

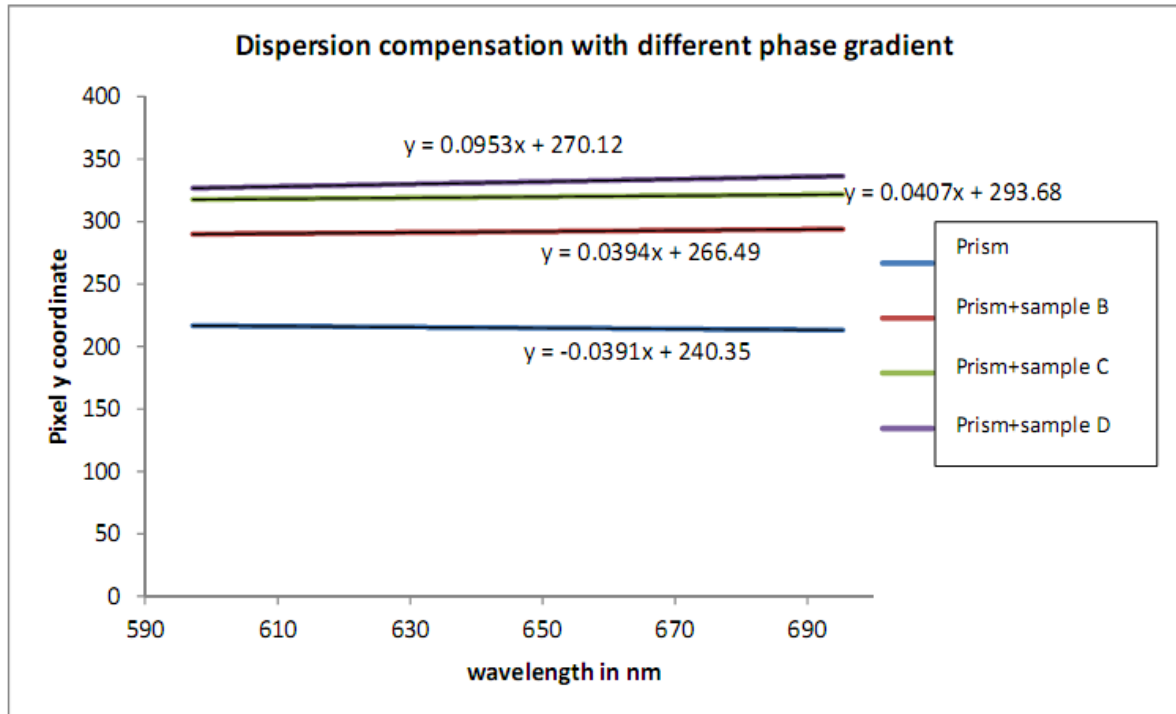


Fig. 5.4 Shown plot compares compensation of prism dispersion with different phase gradient samples in the wavelength range 600-700 nm. The blue line shows prism regular dispersion having a negative slope. An ideally compensated light should have a zero slope so that the deflection angle is constant for all wavelengths. Prism dispersion compensated with sample B of 5×10^{-5} rad/nm phase gradient gives us a slope of 0.0394 which is the best compensation achieved in 600-700 nm bandwidth. Prism dispersion compensated with sample C of 6×10^{-5} rad/nm phase gradient gives us a slope of 0.0407 which is compensating slightly poorly or similar when compared to 5×10^{-5} rad/nm phase gradient. Prism dispersion is over-compensated by sample D of 7×10^{-5} rad/nm phase gradient with a slope of 0.0953. We therefore can see that a phase gradient of 5×10^{-5} rad/nm is best for compensation in 600-700 nm wavelength range.

- Dispersion compensation results for 700-800 nm

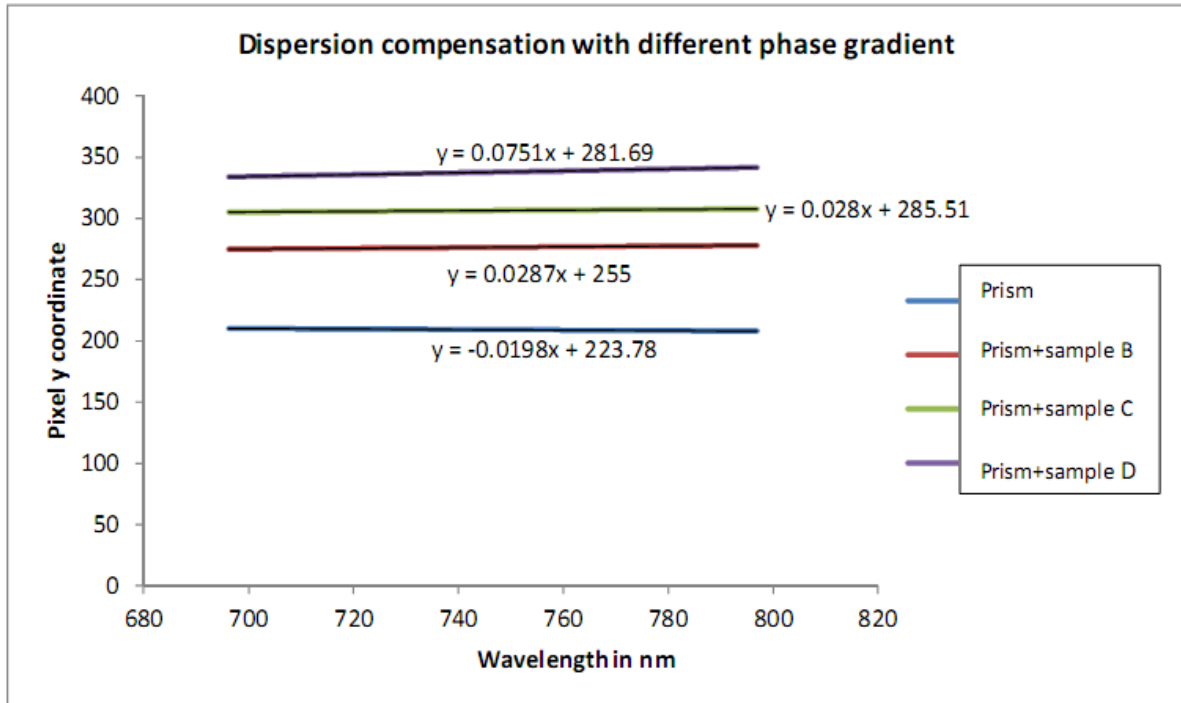


Fig. 5.5 Plot above compares compensation of prism dispersion with different phase gradient samples in the wavelength range 700-800 nm. The blue line shows prism regular dispersion having a negative slope. As we can see, the prism dispersion is getting lesser as we increase the wavelength. It implies that prism dispersion is strong at shorter wavelengths. An ideally compensated light should have a zero slope so that the deflection angle is constant for all wavelengths. Prism dispersion compensated with sample B of 5×10^{-5} rad/nm phase gradient gives us a slope of 0.0287. Prism dispersion compensated with sample C of 6×10^{-5} rad/nm phase gradient gives us a slope of 0.028 which is similar when compared to 5×10^{-5} rad/nm phase gradient. So both sample B and C are giving the best compensation in 700-800 nm. Prism dispersion is over-compensated by sample D of 7×10^{-5} rad/nm phase gradient with a slope of 0.075

Discussion-

Analytically it was observed that a phase gradient value of 6×10^{-5} rad/nm should compensate for the dispersion of glass (here, prism) in the wavelength range 600-800 nm. For dispersion measurements in the wavelength range 500-800 nm, it is observed that phase gradient of 5×10^{-5} rad/nm (sample B) best compensates for prism dispersion. A change in phase gradient is obvious because the slope of the dispersion curve has changed with change in wavelength range.

Though the absolute dispersion of prism+sample B and prism+sample C is less than the dispersion of prism in 500-600 nm, it is still not ideal. Also, sample B and sample C overcompensate for the dispersion in 600-800 nm. Therefore, a phase gradient of value less than 5×10^{-5} rad/nm should do the job of compensating in the range 500-800 nm. Higher phase gradient of 7×10^{-5} rad/nm is bound to overcompensate for prism dispersion in 500-800 nm range. Nonetheless, the analytical approach gave correct order of magnitude in deciding the phase gradient required for achromatic response and the success of this study lies in the fact that we could show the dispersion of material changing its sign due to introduction of metasurfaces.

Chapter 6

Conclusion for Dispersion Compensation

We have successfully demonstrated achromatic behaviour by using a combination of prism and constant phase gradient metasurface in the visible region 500-600 nm. With the choice of correct phase gradient, we can extend our observations to 600-800 nm thereby covering the whole visible range spectrum. More than one prism is generally required to get constant refracted angle at the output for all wavelengths. Here, we do the same job with a single prism coupled with metasurfaces. This indeed promises miniaturization of optical components thereby bringing advancement in the field of flat optics and reducing the size, weight and cost of optical imaging systems.

The unique nature of this study is its simple approach by not considering the single antenna resonance but just utilizing the phase gradient of metasurface to achieve achromatic response. This study can be extrapolated to design a metasurface which in combination with conventional lens acts as achromatic lens and is aberration free, giving super resolved, sub-diffraction imaging in the visible range.

The novelty of this research work lies in the fact that we were able to resolve very small amount of dispersion, calculated values show that we are dealing with angles as small as 0.1-0.2 degree and also measuring very shallow phase gradients of the order of 10^{-5} rad/nm. Thanks to the technique of measuring dispersion in the Fourier space, we could get a handle on quantifying such small quantities.

The limitation of this technique is that the amount of compensated light is low compared to the direct light at $k = 0$. This can be corrected if we fabricate metasurfaces with higher transmission efficiency. Also, a near achromatic condition can be achieved but totally eliminating dispersion is an ideal case owing to the experimental errors

Chapter 7

Ellipsometry

This optical characterization technique is used to probe dielectric properties like refractive index and dielectric function of thin films. A change in the polarization of reflected or transmitted light is the key to investigate such dielectric properties of material and this information is compared to a model. Characterization of roughness, thickness, doping concentration and other such properties of material can be carried out in ellipsometry. When the incident radiation interacts with the material, there is a polarization change in the radiation due to material's properties such as thickness, refractive index or dielectric function tensor. The measurement becomes sensitive to the change in polarization of the reflected/transmitted/scattered light and thus it is used as a signal to measure. The amplitude ratio Ψ and phase difference Δ are used to quantify this polarization change. Excellent resolution to the subnanometer regime can be obtained because ellipsometry makes use of the phase (information about polarization) [27].

The experimental setup involves a linearly polarized light following onto the sample and the reflected light after passing through an analyzer falling onto the detector. Most ellipsometry experiments work in the reflection scheme. p polarized light is the one when polarized light is parallel to the plane of incidence and s polarized light has the polarization direction perpendicular to this plane.

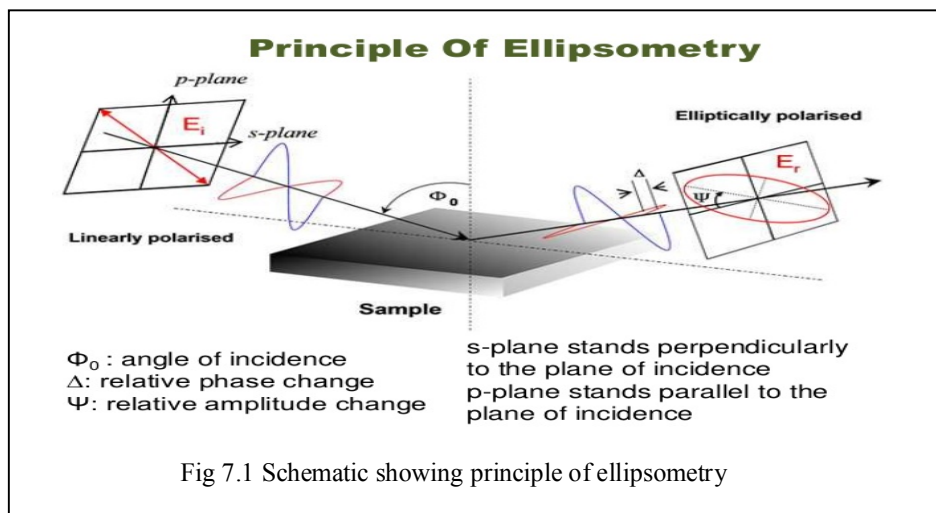
The technique decomposes the s and p components of the reflected light and the amplitudes of these two components are represented by $r(s)$ and $r(p)$ respectively.

The complex reflectance ratio $\rho = r(s)/r(p) = \tan\Psi e^{i\Delta}$ is what is generally measured by ellipsometry. The Ψ and Δ information cannot be directly used to find out optical constants, we use different models to measure optical properties. Cauchy model has six parameters $A_n, B_n, C_n, A_k, B_k, C_k$ which when set to some particular values depending upon the sample shows how good our data agrees with the model.

Cauchy Dispersion formula is given by:

$$n(\lambda) = A + \frac{B}{\lambda^2} + \frac{C}{\lambda^4}$$

k parameters default to zero when there is no absorption by the sample. Therefore, A_k, B_k, C_k take zero value or very small value for samples in most cases.

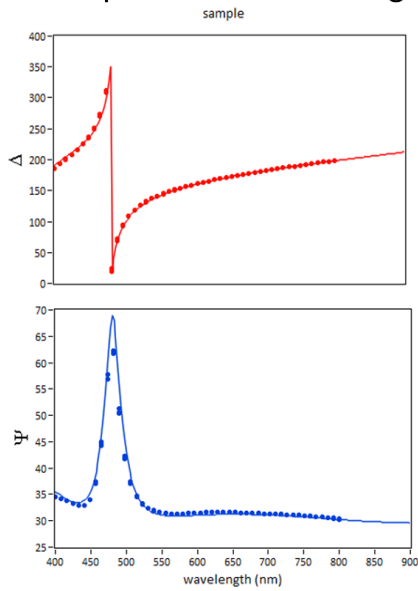


7.1 Dispersion curves of ZnO thin films by ellipsometry

It was initially thought that metasurface samples, concerning the dispersion compensation experiment, were to be fabricated using zinc oxide (ZnO). Measurements on ellipsometry were thus taken to obtain dispersion curves for Gallium doped ZnO. This dispersion data was to be used in FDTD calculations to see phase response of electromagnetic waves passing to ZnO metasurface samples. The choice of material changed when we collaborated with Prof. Federico Capasso's group at Harvard where they fabricated TiO_2 metasurface samples for dispersion compensation experiments. Nonetheless, following dispersion data was obtained for Ga doped ZnO thin films on Si substrate and Cauchy model was used for fitting.

Fig 7.2 Ellipsometry measurements for sample 1 and 2

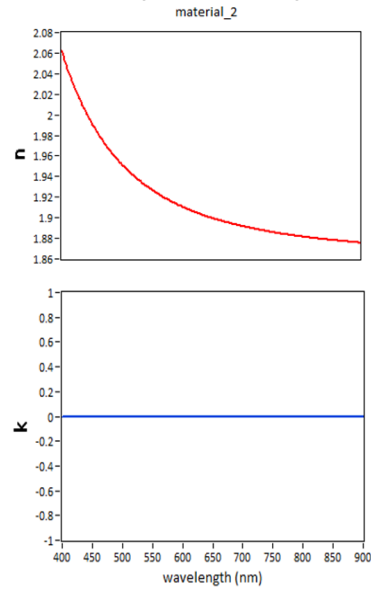
Sample 1- model fitting



Sample-
GZO on Si

Dots- data
Line- Model

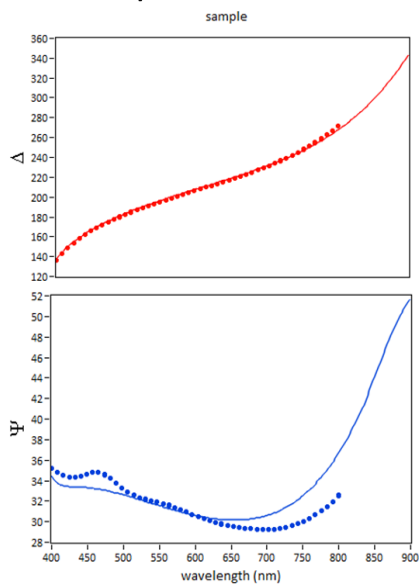
Sample 1- Dispersion curves



Thickness-198.9 nm

Material is transparent as
 $k(\lambda) = 0$

Sample 2- model fitting

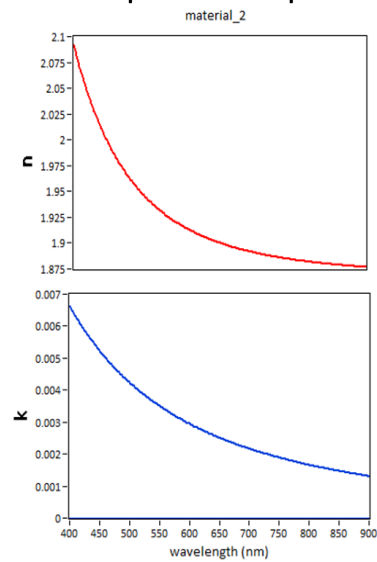


Sample-
GZO on Si

Dots- data
Line- model

This sample has thickness less than 150 nm. Therefore, the curve has shifted compared to other samples and the fit for Ψ is not so accurate

Sample 2- Dispersion curves



Thickness- 133.7 nm

Very less absorption in this sample which decays with wavelength

Chapter 8

Broadband Achromatic Metalens

The analytical method of achieving achromatic response in prism proves motivational in accepting a similar approach to design achromatic metalens in the visible range. This particular problem is still being investigated as a part of the thesis. The idea is to calculate the phase response on a curved interface of a plano convex lens to compensate for chromatic dispersion. If we know the chromatic dispersion of lens, we can ask the question: what is the phase response as a function of wavelength required to completely compensate this dispersion? If this can be found out and proved experimentally, chromatic aberrations will be ruled out thus improving the functionality of lens and enhancing image quality.

A very recent study has shown interesting results for achromatic focusing and imaging in 470-670 nm range where they use nanofin design responsible to tailor dispersion of light [28]. However they report to have an efficiency of 20% at 500 nm. Our study wants to have higher efficiency. Another recent study discusses an analytical approach wherein they add a substrate-corrected phase profile to overcome spherical aberrations [29]. We are more interested in working on chromatic aberrations where the lens does not change focal length upon change of wavelength.

APPENDIX

Fabrication process

1. Electron Beam Lithography (EBL)

Focussed beam of electrons draw desired shapes on a substrate which has a resist. A resist is typically an electron-selective film. By changing solubility of the resist, there is selective removal of either the exposed or non-exposed part by the electron beam when immersed in a solvent. Customized patterns can be drawn in the resist by EBL with resolution on 10 nm and hence such maskless lithography allows for higher resolution while writing patterns.

2. Atomic Layer Deposition (ALD)

Semiconductor device fabrication generally involves ALD. It uses gas phase process sequentially. Two precursors are used. These chemical precursors react one at a time with the targeted surface of the material, in a sequential, self-limiting manner. A thin film is deposited with repeated exposure to separate cursors.

3. Reactive Ion Etching (RIE)

It is a type of dry etching which is used for removing material from a masked pattern when material is exposed to a stream of ions. This bombardment of ions uses chemically reactive plasma generated under low pressure by electromagnetic field.

Finite Difference Time Domain

Finite Difference Time Domain (FDTD) method offers modelling systems involving computational electrodynamics in an extremely simple way. Kane S. Yee had done pioneering work in proposing this method at first. The method adapts a discrete approach to solve an electromagnetic problem wherein it discretizes the Maxwell's equations both in space and time. The electric and magnetic field components are allocated in space and the evolution of the system is observed as marching in time until the behaviour of electromagnetic field evolves fully to show either a transient or a steady-state. Central-difference approximations to the space and time partial derivatives are used while discretizing the time-dependent Maxwell's equations in partial differential form. The resulting finite difference equations are solved in a leapfrog manner. A single simulation run can accommodate a wide range of frequencies because it involves the time-domain method. FDTD works on the grid-based differential numerical modelling methods.

To find out the FDTD solution to figure out electromagnetic response in the given space and ultimately solve Maxwell's equations, it is necessary to specify a computational domain where simulations will be performed. E and H fields are determined at every point in this domain. Also, we must specify the material (dielectric or metal or even) for every cell of this domain. After fixing the computational domain and the grid, we need to insert a source. It can be an applied electric field or an impinging plane wave. Because we can directly determine the E and H, we can get the E and H at any point in the computational domain as an output of the simulation. We thus get the E and H information forward in time. Far field output results can also be obtained using the near-to-far-field transformations.

In our case, we have plane wave as a source, and we pass this wave through metasurface structures of varying geometry to observe the phase response at different points over a large number of wavelengths.

BIBLIOGRAPHY

1. J. B. Pendry, D. Schurig, D. R. Smith, *Controlling Electromagnetic Fields*, Science 312, 1780 (2006)
2. U. Leonhardt, *Optical Conformal Mapping*, Science 312, 1777 (2006)
3. W. Cai, V. Shalaev, *Optical Metamaterials: Fundamentals and Applications* (Springer, New York, 2009)
4. N. Engheta, R. W. Ziolkowski, *Metamaterials: Physics and Engineering Explorations* (Wiley-IEEE Press, New York, 2006)
5. Yu N, P. Genevet, MA. Kats et al, *Light Propagation with Phase Discontinuities: Generalized Laws of Reflection and Refraction*, Science 334(6054), (2011)
6. R. D. Grober, R. J. Schoelkopf, D. E. Prober, *Optical antenna: Towards a unity efficiency near-field optical probe*, Appl. Phys. Lett. 70, 1354 (1997)
7. L. Novotny, N. Van Hulst, *Antennas for light*, Nat. Photonics 5, 83 (2011)
8. Francesco Aieta, Mikhail A. Kats, Patrice Genevet, Federico Capasso, *Multiwavelength achromatic metasurfaces by dispersive phase compensation*, Science 347, 1342 (2015)
9. F. Aieta, P. Genevet, N. Yu, M.A. Kats, Z. Gaburro, F. Capasso, *Out-of-plane Reflection and Refraction of Light by Anisotropic Optical Antennas Metasurfaces with Phase Discontinuities*, Nano Lett. 12, 1702 (2012)
10. X. Ni, N. K. Emani, A. V. Kildishev, A. Boltasseva, V. M. Shalaev, *Broadband light bending with plasmonic nanoantennas*, Science 335, 427 (2012)
11. D. Lin, P. Fan, E. Hasman, M. L. Brongersma, *Dielectric gradient metasurfaces optical elements*, Science 345, 298 (2014)
12. F. Aieta, Patrice Genevet, Mikhail A. Kats, Nanfang Yu, Romain Blanchard, Zeno Gaburro, Federico Capasso, *Aberration-free Ultrathin Flat Lenses and Axicons at Telecom Wavelengths based on Plasmonic Metasurfaces*, Nano Lett. 12, 4932 (2012)

13. A. Pors, M. G. Nielsen, R. L. Eriksen, S. I. Bozhevolnyi, *Broadband Focusing Flat Mirrors Based on Plasmonic Gradient Metasurfaces*, Nano Lett. 13, 829 (2013)
14. S. Vo, David, Fattal, Wayne V. Sorris, *Subwavelength Grating Lenses with a Twist*, IEEE Photon Technol. Lett. 26, 1375 (2014)
15. F. Aieta, P. Genevet, M.A. Kats, F. Capasso, *Aberration of flat lenses and Aplanatic metasurfaces*, Optics, Express, Vol. 21, Issue 25 (2013)
16. Ehsan Arbabi, Andrei Faraon et al, *Controlling the sign of chromatic aberration in diffractive optics with dielectric metasurfaces*, Optics, Vol 4, Issue 6 (2017)
17. M. Khorasaninejad, Z. Shi, A. Y. Zhu, W. T. Chen, V. Sanjeev, A. Zaidi, F. Capasso, *Achromatic Metalens over 60 nm Bandwidth in the Visible and Metalens with Reverse Chromatic Dispersion*, Nano Lett. 17 (3), (2017)
18. R. C. Devlin, M. Khorasaninejad, W. T. Chen, J. Oh, F. Capasso, *High Efficiency dielectric metasurfaces at visible wavelengths*, Proc. Nat. Acad. Sci. USA, 113, 10473 (2016)
19. M. Khorasaninejad, W. T. Chen, A. Y. Zhu, J. Oh, R. C. Devlin, C. R. Carmes, I. Mishra, F. Capasso, Fellow, IEEE, *Visible Wavelength Planar Metalenses Based on Titanium Dioxide*, IEEE Journal of Selected Topics in Quantum Electronics, 23, No. 3, May/June 2017
20. J. A. Kurvits, M. Jiang, R. Zia, *Comparative analysis of imaging configurations and objectives in Fourier Microscopy*, Journal of the Optical Society of America A, Vol. 3, 11 (2015)
21. A. Grbic and C. Pfeiffer, *Metamaterial Huygen's surfaces: Tailoring wave fronts with reflectionless sheets*, Phys. Rev. Lett. 110, 197401 (2013)
22. Yan Zhang, Jiasheng Ye, Dan Hu et al, *Terahertz super thin planar lenses*, Proc SPIE 8562, Infrared, Millimeter wave and Terahertz technologies II (2012)
23. Francesco Aieta, Mikhail A. Kats, Patrice Genevet, Reza Khorasaninejad, Federico Capasso, *Achromatic metasurfaces enable multi-wavelength flat optical components: demonstration of a dispersion-less beam deflector*, CLEO (2015)
24. P. Genevet, N. Yu et al, *Ultra-thin plasmonic optical vortex plate based on phase discontinuities*, Applied Physics Letter 100 (1), 013101 (2012)
25. N. Yu, F. Aieta, P. Genevet, M.A. Kats, Z. Gaburro, F. Capasso, *A broadband, background-free quarter-wave plate based on plasmonic metasurfaces*, Nano letters 12 (12), 6328 (2012)
26. P. Genevet, F. Capasso, *Holographic optical metasurfaces*, Reports on Progress in Physics 78 (2), 024401 (2015)

27. I. Ohlidal and D. Franta, *Ellipsometry of thin film systems*, Progress in Optics, vol. 41, ed E. Wolf, Elsevier, Amsterdam, 2000
28. W.T. Chen, A.Y. Zhu, V. Sanjeev, M. Khorasaninejad, Z. Shi, E. Lee, F. Capasso, *A broadband achromatic metalens for focusing and imaging in the visible*, Nature Nanotechnology O, o (2018)
29. B. Groever, C. Roques-Carmes, S. J. Brynes, F. Capasso, *Substrate aberration and correction for meta-lens imaging: an analytical approach*, Applied Optics O, o (2018)